International Journal of
Air-Conditioning and Refrigeration

RESEARCH Open Access

Implementation of phase change material for cooling load reduction: a case study for Cairo, Egypt

Joseph Alfy Kamel*, Ehab Mouris Mina and Ahmed Moneeb Elsabbagh

Abstract

Integrating a phase change material (PCM) into building envelopes can reduce energy needs in the built environment, and the consequent greenhouse emissions. This research examines the impact of PCM integrated into a traditional wall in Egypt on peak and average cooling energy consumption. A MATLAB code based on the finite volume technique using the Crank-Nicolson method for discretization is implemented. Several benchmark cases and experimental results validate the code. The time-dependent boundary conditions of the cases examined were based on the irradiance and ambient temperatures measured in Cairo, Egypt. Simulations are performed on eight different PCMs, using their real published DSC curve. The study aims to investigate the performance of each PCM at different positions, thicknesses, and wall orientations. The calculations revealed that using the proper PCM type and the proper position could decrease the average by 38.14%, Also the peak heat flux could be decreased by 58.53%.

Keywords: Phase change material, Building envelope, Latent heat storage, Infinite volume method

1 Introduction

World energy consumption has increased dramatically in recent decades as a result of population expansion, and the increase in the standard of living. According to recent study by British petroleum [9], the global annual growth rate of primary energy consumption is 1.6%. The study also shows that in Egypt the Primary energy consumption growth rate per year is 2.7%. Buildings account for a third of the world's greenhouse gas emissions and more than 40% of the energy used globally. Electricity consumption in buildings is thought to have increased emissions at a rate of 1.7% per year for residential structures and 2.5% per year for commercial buildings [41], Also, Egypt's climate is changing in terms of high and low temperatures. Where Global warming raise the high summer temperatures which increase the cooling energy required [15] and because buildings have a relatively long lifespan, actions made now will have an extended impact on the energy consumption and greenhouse gas emissions.

One of these actions is to decrease the cooling load to reduce the energy consumed for air conditioning unit. The construction of the building envelope is critical in influencing the building's thermal performance and energy consumption, where the building envelope acts as a barrier to external influences such as periodic changes in ambient temperature and the solar irradiance on external walls. To help achieve the objective of lowering energy usage in buildings, several new technologies are developed. Some of these technologies are concerned with thermal insulation in building envelopes [3]. Another technique is the use of thermal energy storage materials. Thermal energy storage systems are divided into two types: sensible heat storage and latent heat storage.

Several research papers have adopted the increase in the envelope thermal resistance as a strategy to reduce the cooling load, and consequently the building energy use. Baetens et al. [5] found that the energy usage

*Correspondence: joseph.alfy@eng.asu.edu.eg

Mechanical Department, Faculty of Engineering, Ain Shams University, Cairo, Egypt

decreased as an effect of integrating gas-filled panels in buildings. In other studies, Vacuum insulation panels (VIPs) have shown a high-performance as thermal insulation for construction applications [4, 20, 34]. Also, Aerogels are applied as thermal insulation [4, 19].

Another approach is to implement a material to add a storage effect to the thermal resistance effect. Phase change materials 'PCMs', work on the premise of thermal energy storage via latent heat. It has a great energy density storage at a range around the melting point [11]. PCMs undergo a phase transition at a nearly constant temperature from solid to liquid during this period (charging), it absorbs high thermal energy. This stored energy is released back during solidification (discharging). They appear to be reducing cooling energy usage and peak cooling loads, as well as deferring peak loads to later hours [7, 17, 28, 40].

Many studies are made to investigate the impact of implementing a PCM layer into a wall on the cooling load reduction. Conrad Voelker et al. [43] employed an experiment near Weimar, Germany, where both paraffin and a salt mixture are applied in a room wall. To enhance the thermal mass of the wall and, as a result, the maximum room temperature decreased by 4 °C. In another study, Lv Shilei et al. [33] performed an experiment held in Shenyang, in northeast China, to investigate the impact of PCM on the thermal heat flow to a room in winter. A phase change wall room was formed by sticking a PCM (capric acid and lauric acid mixture) and gypsum boards on the surface of an ordinary room wall. The results show that the heat flow through the south wall of the ordinary wall room varied from 34 to 60 W/m^2, while in the case of the phase change wall room the heat flow varied from 33 to 52 W/m^2. Also in the city of Aveiro in Portugal, António Figueiredo et al. [16] conducts an experiment, utilizing two rooms, one of which has PCM panels placed into a gypsum board wall panels. The results of the room measurements revealed that using PCM in one of the rooms reduced overheating by 7.23%. In another research, Myriam Bahrar et al. [6] performed an experimental test in which a guarded hot box used to perform thermal tests in real weather condition. Experiment revealed a 1.7 °C drop in the highest interior surface temperature. Moreover, peaks are shifted of about 2 h with night ventilation. Another experimental work undertaken in the Iraqi City of Diwaniya intends to analyze and investigate the application of PCM capsules as an insulating material into the hollow bricks that construct a wall. Two similar rooms were conceived and built to test two southern walls with and without PCM in their natural outside environment. The results reveal that encapsulating PCM in the treated wall reduces the inner surface wall and room temperature by approximately 4.7°°C while increasing the time lag by 2 h [1].

To choose the proper phase change material, you must first determine the wall composition, exterior building walls orientation, PCM layer location in the wall, and the time of year during which the PCM is expected to lower the building's thermal load. These variables will influence the PCM selection as described in many articles [18, 21, 25, 29]. But the most critical parameter that affects the PCM selection is the building's location where the solar irradiance change according to changing the altitude of the country. A numerical study [2] aimed to examine the impact of PCM on the thermal performance in the three cities of Diyarbakir, Konya, and Erzurum in Turkey and to detect the proper thickness and melting temperature of PCM in a wall composed of interior plaster (20 mm), concrete (250 mm), insulation (20 mm), and exterior plaster (8 mm) for best thermal performance. Calculation results show that placing the PCM in between insulation and the external plaster saves the most energy under heating settings. Placing PCM between the inner plaster and concrete saves the most energy under cooling circumstances. The yearly optimal PCM melting temperatures for Diyarbakir, Konya, and Erzurum are 20 °C, 25 °C, and 16 °C, respectively. Another numerical research is performed using EnergyPlus to evaluate the impact of integrating a PCM layer in a traditional building envelope for eight different cities. Thirteen different PCMs with melting temperatures ranging from 20 to 32 °C were studied, and the results show that For Abu-Dhabi, Dubai, Faisalabad, Mecca, Nouakchott, Jodhpur, Cairo, and Biskra, the best thermal performance was found when a PCM with a melting point at 27, 27, 29, 27, 31, 32, 20, and 21 °C, respectively [37]. Another study investigated the impact of PCM on energy savings. Seven different cities were chosen to represent the major European climatic zones, and the cases were solved by employing six different PCMs with melting peak temperatures ranging from 18 to 28 °C. The results show that the ideal melting peak temperature of the PCM is greater in warmer climates between 22 and 26 °C, compared to 18 to 24 °C in colder climes. It is also established that the energy-saving impact is stronger in warmer climates [35]. In another research in New Delhi, a study on cooling load reduction with three commercially available PCMs (HS29, OM32, and HS34) installed into a building envelope was conducted. According to the results, HS34 with a melting temperature of 34 °C is the appropriate PCM for New Delhi under the design parameters [32].

As mentioned before, the PCM position in the wall is a critical parameter; if the melting temperature of the PCM is low, the proper location should be close to the side of lower temperature; also, if the melting

temperature is high, the PCM position should be close to the high side temperature to ensure that the PCM perform the charging and discharging cycle. To explore the influence of PCM location on thermal comfort in the interior of the building, an experimental investigation involving a construction of a model of constructing wall segments and to facilitate one-dimensional heat conduction through the building wall fragment, the model was insulated with wood. The model was made up of two water baths. In one of the water baths, a heating system was constructed, and water was held at room temperature in the other one. The results demonstrate that placing a two inch thick layer of paraffin wax type P56-58 closer to the heat source leads to a lesser temperature increase in the cold water bath than placing the PCM layer closer to the heat sink [22]. Another research evaluated the impact of adding thirteen different phase change materials into traditional building walls in Isfahan, Iran. The base wall from the interior was composed of plaster (20 mm), clay brick (150 mm), and cement (30 mm). The effect of PCM location within the wall on heat transmission was evaluated in two ways: PCM layer between plaster and brick, and PCM layer between brick and cement. The calculations revealed that using the proper PCM type and the proper position could decrease the heat flux by 16.95%, 30.20%, and 47.58% for thicknesses of 1 cm, 2 cm, and 4 cm, respectively [26].

However, as mentioned before it is critical to choose the right PCM type based on the wall orientation where the solar radiation changes on each wall orientation. A study aimed to investigate the effect of PCM on cooling load reduction by implementing a PCM layer into different wall orientations, the results show that a certain PCM cannot be chosen as the best choice without specifying the wall orientation first, for a given climate, we can choose the proper PCM only after comparing the performances of the PCMs in all relevant orientations [30].

Depending on the literature review, the current research fills the gap in two areas. First, the optimum PCM is highly dependent on the environmental conditions (solar irradiance and ambient temperature). This research considered a validated model for solar irradiance and acceptable distribution for ambient temperature in Cairo, Egypt. Also, the typical wall construction was used as a base wall. Therefore, the results are tangible to the application in Cairo and similar cities. Second, this study considered the real dependence of specific heat on temperature as obtained from differential scanning calorimetry (DSC). The results of this research could be used to validate any approximation of the specific heat.

2 Model description

The effect of adding a PCM layer to a typical wall used in construction in Cairo, Egypt, is studied numerically. Several walls having a PCM layer at different position inside the wall were studied. A MATLAB code is used to solve the heat diffusion equation through several layers of construction material under real conditions representing the Summer and Winter design day in Cairo.

The following assumptions were considered in the mathematical model:

- Conduction heat transfer is assumed to be unidimensional.
- There is no contact resistance between different layers of the composite wall.
- For each wall material, the thermo-physical properties are assumed to be constant except for the phase change materials layer, since their properties depend on the liquid and solid phases, as well as the temperature.

2.1 Building envelope

In this study, one of widely used external building wall in Egypt is chosen to be our base wall (without PCM) which consists of four layers; interior mortar (25 mm), two layers of brick each on had thickness of (65 mm), and exterior mortar (25 mm).

The thermal properties of components of the external building wall are listed in Table 1 [14]

2.2 PCM

To analyze the contribution efficiency of the PCM layer by the comparison, two walls were built as shown in Fig. 1. One was the base wall, while others were the wall with a PCM layer.

Three different scenarios of integration of PCM to the base wall were considered:

- Locating PCM between the brick and exterior mortar.
- Locating PCM between the brick and interior mortar.
- Locating PCM between the two layers of the brick.

Table 1 Thermal properties of wall material

Materials	K (W/mK)	Density (kg/m3)	C (J/kgK)
Mortar	1.4	2162	920
Brick	0.7	1300	840

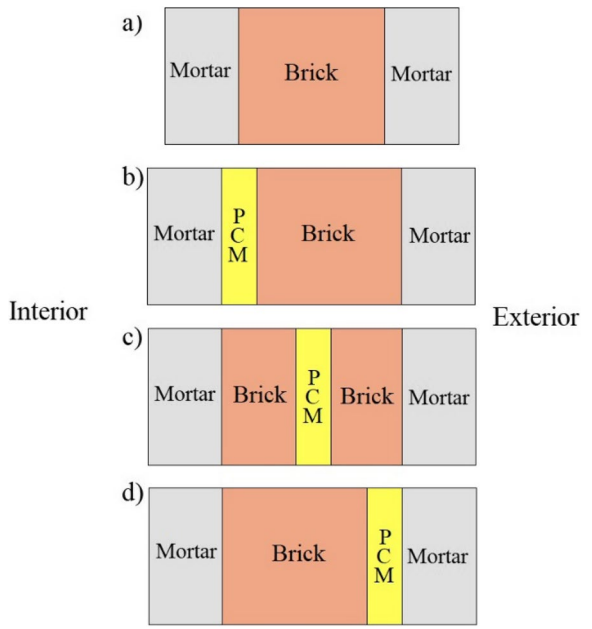

Fig. 1 Wall composition. **a** Base wall. **b** Inner PCM wall. **c** Middle PCM wall. **d** Outer PCM wall

In our study, the heat capacity approach was employed to model the heat transfer caused by phase transition. Eight different PCMs with melting temperatures varies from 24 to 35 °C will be used in this research their properties and the heat capacity curves are shown in Fig. 2 [24, 27, 31, 38, 39, 42, 44].

3 Governing equations

The governing equation for one-dimensional, transient heat conduction for PCM and for other wall components can be expressed by

$$\frac{\partial \mathrm{T}}{\partial \mathrm{t}} = \alpha \frac{\partial^2 \mathrm{T}}{\partial \mathrm{x}^2} \text{ and } \alpha = \frac{k}{\rho\, C}$$

where α is the thermal diffusivity, k is thermal conductivity, ρ is the density, and C is the heat capacity of the wall material.

3.1 Wall discretization

By discretizing the wall to several nodes as shown in Fig. 3 where the distance between nodes is taken to be equal 1 mm an energy balance is applied for each node, the studied node has given a suffix m and its right node has a suffix m + 1 and the left one has suffix m − 1.

The energy balance result in four equations:

For an interior surface node '*m*' the heat flow to it is by conduction from the neighbor node and a convection from the air in the room this result to change the temperature of the node from ${T_m}^p$ to ${T_m}^{p+1}$

All this could be represented in the next equation

$$\frac{k_{\text{mortar}}}{\Delta x}\left(\frac{{T_{m-1}}^p + {T_{m-1}}^{p+1}}{2} - \frac{{T_m}^p + {T_m}^{p+1}}{2}\right) + h_i\left(T_{\infty,i} - \frac{{T_m}^p + {T_m}^{p+1}}{2}\right) = \rho_{\text{mortar}} C_{\text{mortar}} \frac{\Delta x}{2} \frac{{T_m}^{p+1} - {T_m}^p}{\Delta t}$$

Where $T_{\infty,\,i}$ is the building temperature which chosen to be equal to 25 °C, h_i is the room convection coefficient, Δx is the distance between nodes in the heat flow direction which equal to 1 mm, $\Delta\tau$ is the time step equal to 1 min also, k_{mortar}, ρ_{mortar} and C_{mortar} are the thermal properties of the inside layer of the composite wall which is mortar in our case.T^{P} represents the node temperature at time p and $\mathrm{T}^{\mathrm{P+1}}$ represents the node temperature after time step Δt.

For the interior nodes the heat flow is by conduction from the neighbor nodes which represented in the next equation

$$\frac{k}{\Delta x}\left(\frac{{T_{m-1}}^p + {T_{m-1}}^{p+1}}{2} - \frac{{T_m}^p + {T_m}^{p+1}}{2}\right) + \frac{k}{\Delta x}\left(\frac{{T_{m+1}}^p + {T_{m+1}}^{p+1}}{2} - \frac{{T_m}^p + {T_m}^{p+1}}{2}\right) = \rho C \Delta x \frac{{T_m}^{p+1} - {T_m}^p}{\Delta t}$$

Where k, ρ, and C are the thermal properties for the layer material.

For the node at the interface between two different materials, the heat flow is from the conduction from the neighbor nodes and the energy balance could be written as follows:

$$\frac{AK_a}{\Delta x_a}\left(\frac{{T_{m-1}}^p + {T_{m-1}}^{p+1}}{2} - \frac{{T_m}^p + {T_m}^{p+1}}{2}\right) + \frac{Ak_b}{\Delta x_b}\left(\frac{{T_{m+1}}^p + {T_{m+1}}^{p+1}}{2} - \frac{{T_m}^p + {T_m}^{p+1}}{2}\right) = \left(\rho_a c_a A \frac{\Delta x_a}{2} + \rho_b c_b A \frac{\Delta x_b}{2}\right) \frac{{T_m}^{p+1} - {T_m}^p}{\Delta t}$$

Where subscript a and b are representing the two materials that the interface node is lay between them.

For the exterior surface node, the heat flow to the node from next node at the outer layer of the wall by conduction, convection heat transfer from the ambient and the solar radiation

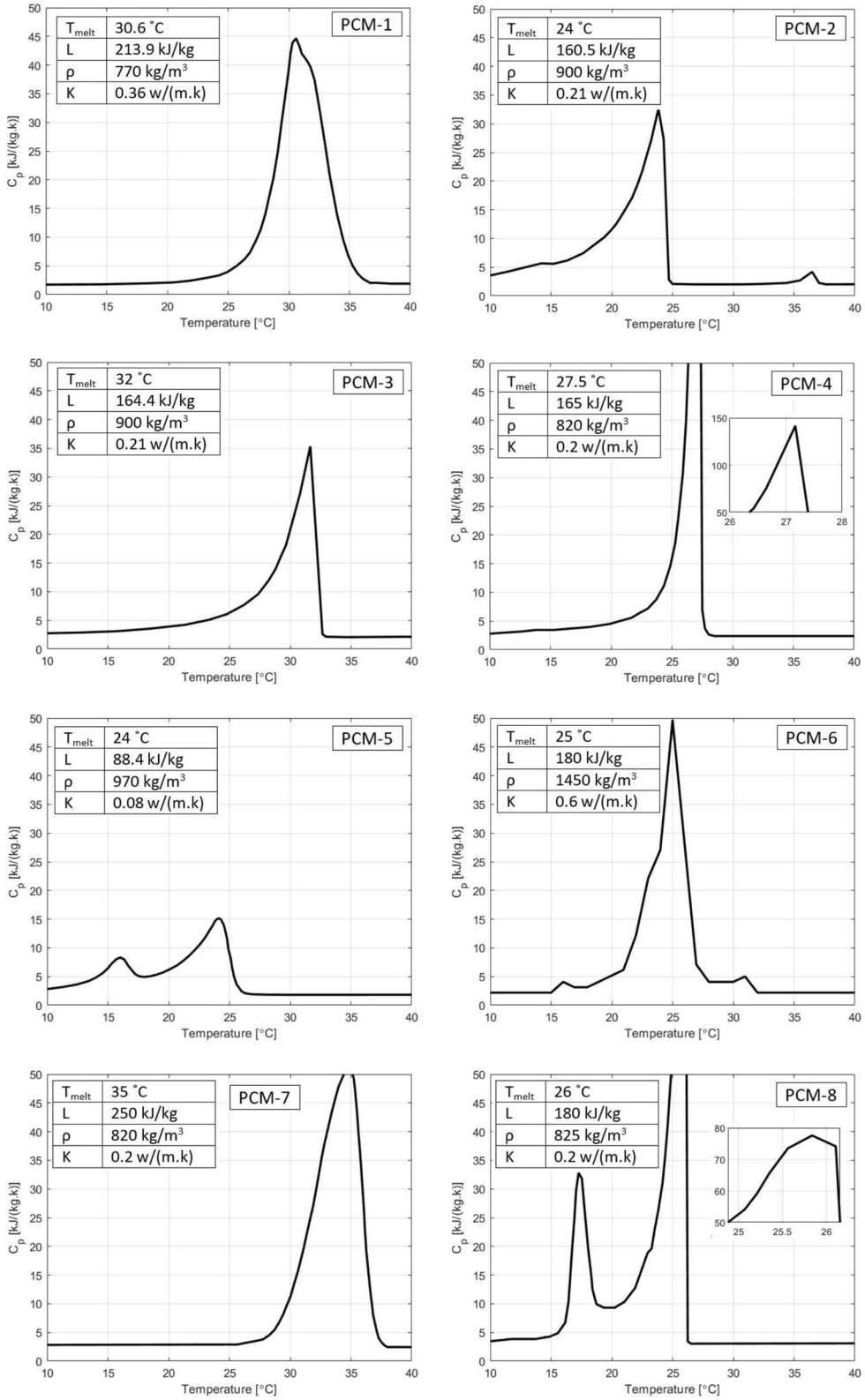

Fig. 2 Specific heat capacity curves for eight different PCMs

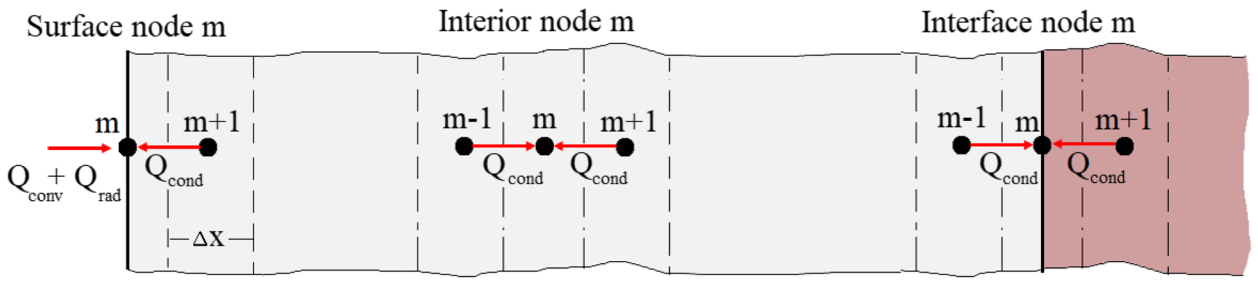

Fig. 3 Surface, interior, and interface nodes in a composite wall

$$\frac{k_{\text{mortar}}}{\Delta x}\left(\frac{{T_{m+1}}^{p}+{T_{m+1}}^{p+1}}{2}-\frac{{T_m}^{p}+{T_m}^{p+1}}{2}\right)+h_o\left(\frac{{T_{\infty,o}}^{p}+{T_{\infty,o}}^{p+1}}{2}-\frac{{T_m}^{p}+{T_m}^{p+1}}{2}\right)+Q_{\text{rad}}=\rho_{\text{mortar}}C_{\text{mortar}}\frac{\Delta x}{2}\frac{{T_m}^{p+1}-{T_m}^{p}}{\Delta t}$$

Where Q_{rad} is the solar radiation.

3.2 Boundary conditions

3.2.1 Solar model

The total incidence radiation on the external surface of the wall has the most influence on the cooling and heating load. To calculate the total incidence radiation on the external surface of the wall, the following equations were used which are converted to a vectorized MATLAB form.

The hour angle can be obtained from the following equation:

$$\omega = (solar\ time - 12) * 15$$

Declination angle obtained from the following formula:

$$\delta = 23.5\ \sin\frac{360(284+n)}{365}$$

Where n is the number of a day in the year

And zenith angle which is the angle of the beam radiation on a horizontal surface obtained by the following equation

$$\theta_z = \cos^{-1}(\sin\delta\sin\varphi+\cos\delta\cos\varphi\cos\omega)$$

Where ϕ is the latitude angle, for Cairo $\phi = 30°$

The incidence angle on the external surface could be obtained using the following formula

$$\theta = \cos^{-1}(\cos\delta\sin\varphi\cos\gamma\cos\omega+\cos\delta\sin\gamma\sin\omega-\sin\delta\cos\varphi\cos\gamma)$$

Where γ is the surface azimuth angle.

The beam radiation is calculated from the formula below:

$$Q_{\text{beam}} = \frac{A_q\ C_n\ \cos\theta}{e^{\frac{B_q}{\cos\theta_z}}}$$

The diffuse radiation is calculated from

$$Q_{diffuse} = \frac{C_q\ A_q}{2\ C_n\ e^{\frac{B_q}{\cos\theta_z}}}$$

And for the reflected radiation

$$Q_{\text{reflected}} = \frac{\rho_{\text{ground}}\ A_q\ C_n\left(C_q+\cos\theta_z\right)}{2\ e^{\frac{B_q}{\cos\theta_z}}}$$

Where A_q, B_q, and C_q are constant.

Where C_n is the clearness index for Cairo [13] and its value for each month is given in Fig. 4.

Finally, the total incidence radiation can be calculated as follows:

$$Q_{rad} = Q_{beam} + Q_{diffuse} + Q_{reflected}$$

Values of average monthly solar radiation obtained from the simulation were compared to the values of the PVWatt calculator which developed by the National Renewable Energy Laboratory (NREL) [12] are given in Fig. 5.

Finaly, the solar irradiance over an average day in june for different oriantaions is obtaind using the simulation as shown in Fig. 6.

3.2.2 Exterior and interior temperatures

The interior temperature is kept at a comfortable level, which has been set at 25 °C, and for the exterior temperature has a periodic value which has a maximum

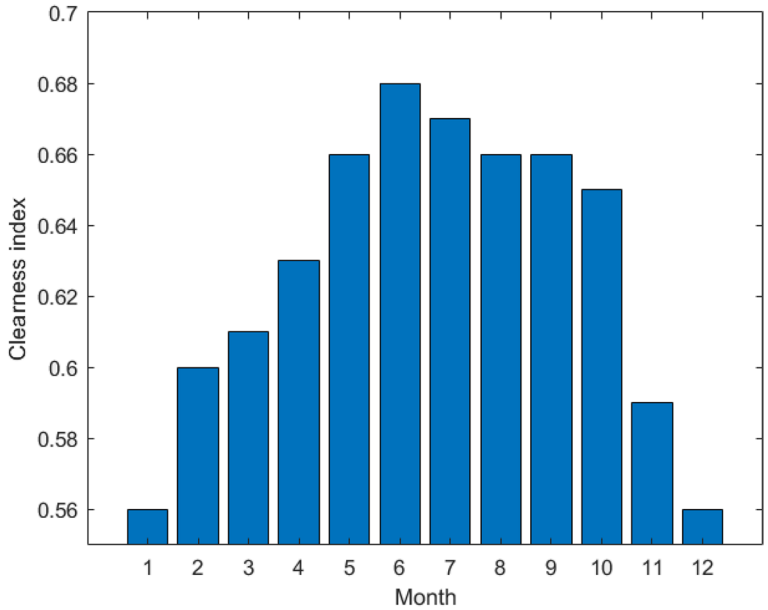

Fig. 4 Clearness index for Cairo

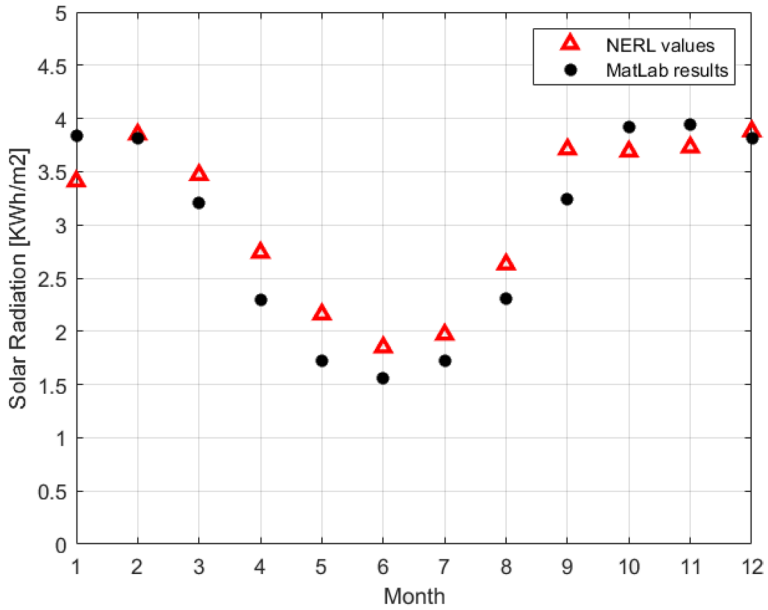

Fig. 5 NERL values vs. MATLAB results

temperature of 35 °C and daily range 13 °C in June and has a maximum temperature of 19 °C and daily range 9 °C in January [10]. Also, the heat transfer convection coefficients are 8 and 17 W/m^2K for inside the room and outside the room respectively. The exterior temperature variations are shown in Fig. 7.

3.3 Numerical model

As shown in Fig. 8, the flowchart shows the algorithmic method used in this study. The heat balance on each node equation is discretized using the Crank-Nicolson method and solved by MATLAB software, the variables as the composite wall layers material and thickness, the boundary

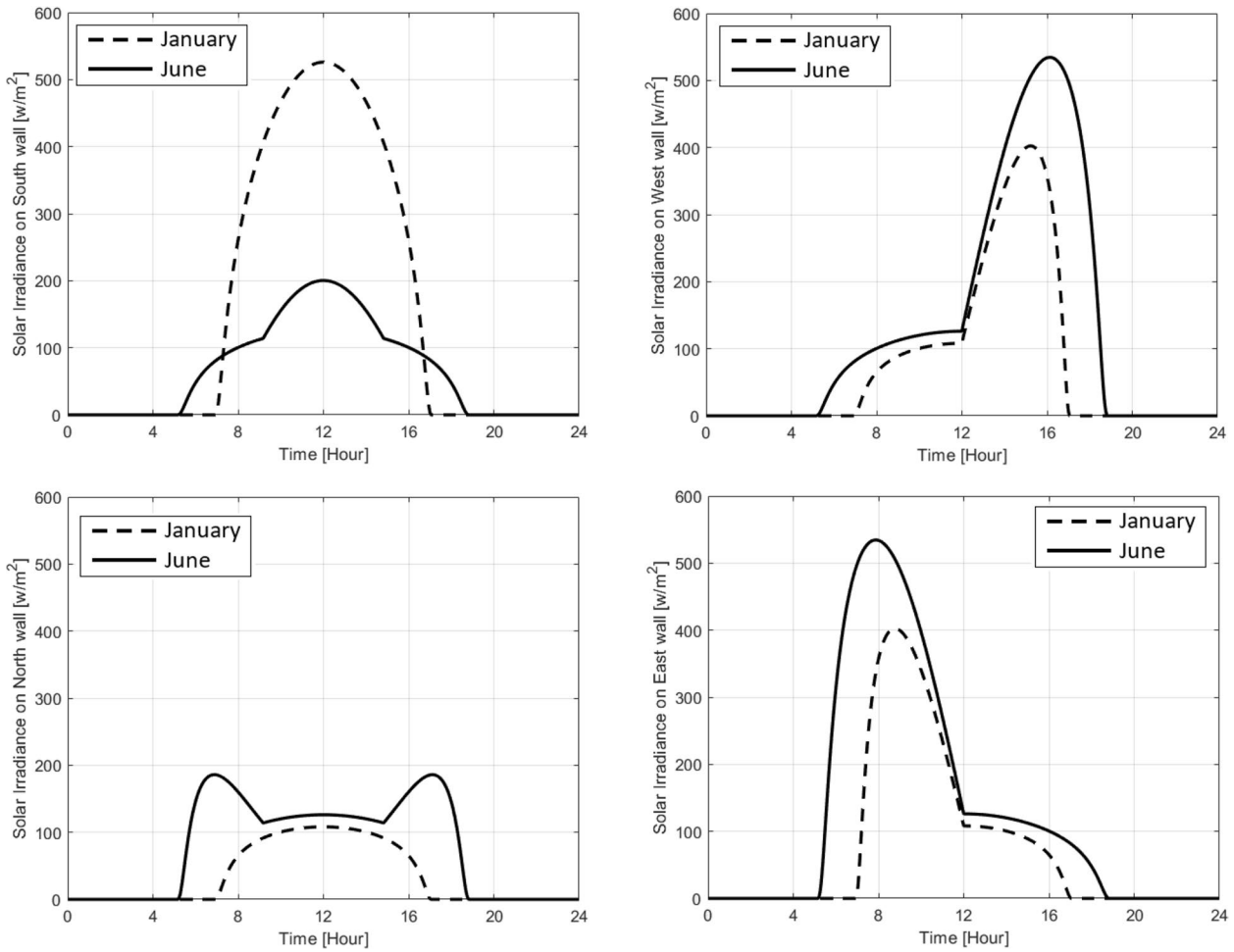

Fig. 6 Solar radiation in June and January at different orientations

conditions, and the initial temperature of the wall are the program inputs, after solving the equations over a day those calculations was repeated for five consecutive days to ensure that the initial condition has no effect on the final results.

The average heat transferred to the room with PCM is determined by summation the heat flux on the inner wall with PCM over the day, and the same method used to determine the average heat transferred to the room in case of a base wall.

Where $T_{s,i,PCM}$ is the temperature of the inner surface of the wall with PCM and $T_{s,i,}$ is the temperature of the inner surface of the base wall.

Our method to investigate the impact of inserting the PCM layer into the wall is by comparing the average heat flow to the room in the case of a wall with PCM layer with the heat flow to the room in the case of the base wall, where the reduction in heat flow represents the reduction in power consumption to keep the

$$\text{Average heat to the room with PCM} = \frac{\sum_{p=0}^{p=1440} h_i \left(\frac{T_{s,i,PCM}^{p+1} + T_{s,i,PCM}^{p}}{2} - T_{\infty,i} \right) * \Delta t}{1440}$$

$$\text{Average heat to the room without PCM} = \frac{\sum_{p=0}^{p=1440} h_i \left(\frac{T_{s,i}^{p+1} + T_{s,i}^{p}}{2} - T_{\infty,i} \right) * \Delta t}{1440}$$

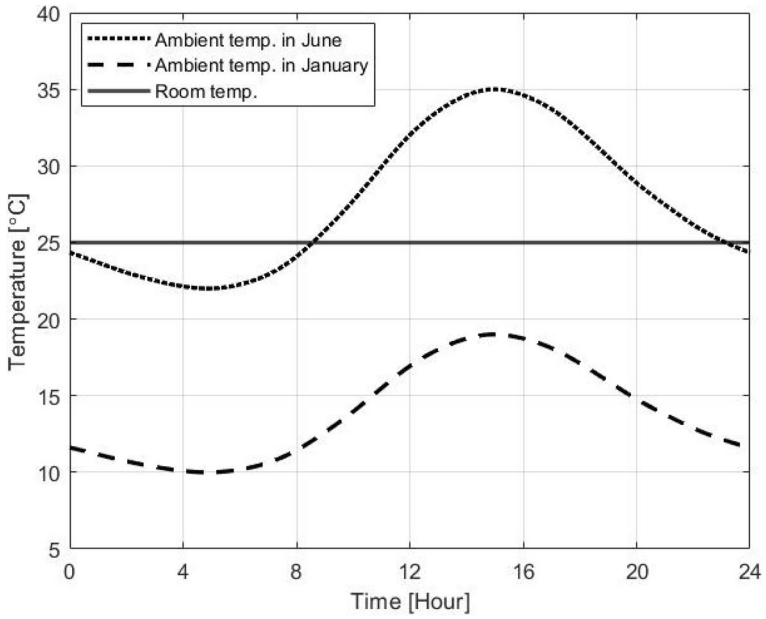

Fig. 7 Exterior temperature variation

building in the comfort range. Another way to evaluate the impact of the PCM layer is by calculating the percentage reduction in maximum heat flow to the room which will impact the maximum capacity of the cooling unit in the building. The formulas used to calculate the percentage reduction in average and peak heat flow to the room are given below.

$$\text{Average heat reduction } \% = \frac{\text{Average heat to the room without PCM} - \text{Average heat to the room withPCM}}{\text{Average heat to the room without PCM}} * 100$$

$$\text{Peak heat reduction } \% = \frac{\text{MAX}\left(\frac{T_{s,i}^{p+1}+T_{s,i}^{p}}{2} - T_{\infty,i}\right) - \text{MAX}\left(\frac{T_{s,i,PCM}^{p+1}+T_{s,i,PCM}^{p}}{2} - T_{\infty,i}\right)}{\text{MAX}\left(\frac{T_{s,i}^{p+1}+T_{s,i}^{p}}{2} - T_{\infty,i}\right)} * 100$$

4 Validation

In this section, we present several numerical and experimental validation examples to demonstrate the applicability of our results.

4.1 Comparison of numerical results with the exact solution for a base wall and PCM wall

The exact solution [8] is used to validate the MATLAB code which solve the governing equations given above to obtain the temperature variation across the base wall with respect to the time. Grid size 1 mm and time step 1 min are taken for a 30-cm-thick brick wall with inner and outer convection coefficients equal to 18 w/m^{2}k and ambient temperature 40 °C. The temperature variation across the wall after 5, 100, 300, and 500 min are plotted for the exact and the program solution, the program results are identical to the exact solution results as shown in Fig. 9.

The PCM layer also verified with an exact solution developed by Solomon [36], a semi-infinite slab paraffin wax laywer at 21 °C initial temperature, The external surface temperature is suddenly risen to 95 °C. The exact solution results after 60 min are compared to the program solutions and plotted as shown in Fig. 10, the results show a good agreement between the exact and the program solution.

4.2 Comparison of simulation result with an experimental result

The numerical method in this paper has been verified by the experimental unit conducted by Yassine Kharbouch

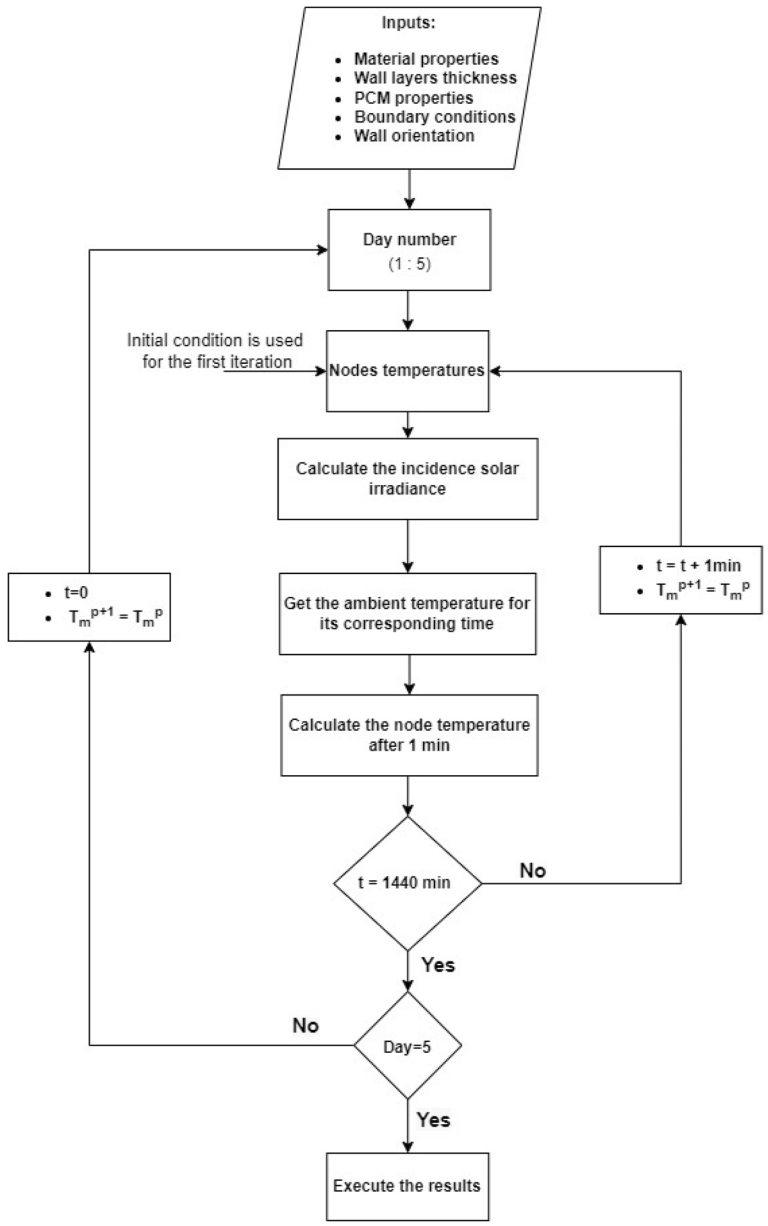

Fig. 8 Flow chart for the used program

et al. [23], a small-scale experimental device has been built, which consists of two identical enclosures separated by a two layers composite wallboard one layer is a 5-mm-thick PCM panel has the following properties as shown in Table 2

And the other layer is a 35-mm-thick wood-based material panel which has the following thermo-physical properties Table 3

The first enclosure is maintained at a nearly constant temperature of about 21 °C, while the second enclosure is exposed to a periodic temperature variation over 480 min.

The temperature data are measured for the interior, interface, and exterior surfaces. The experimental results comparing to the result of our program is shown in Fig. 11, and it is clear that the model and the experimental results are in a good agreement.

5 Results and discussion

5.1 Effect of the presence of PCM in the wall

PCMs were added as a middle layer to a wall with West orientation. The effect of installing different types of

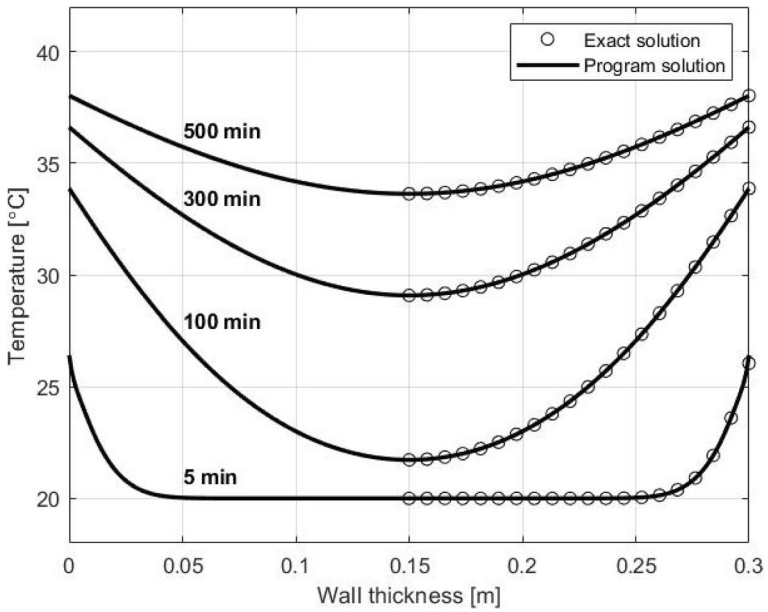

Fig. 9 Exact vs. program solution for a conventional wall

Table 2 Properties of the PCM panel used in the experiment

Melting temp.	21.7 °C
Latent heat	170 kJ/kg [from 14 °C to 30 °C]
Density	680 kg/m^3
Conductivity	0.14–0.18 w/mk

Table 3 Properties of the wood-based material used in the experiment

Heat capacity	2400 J/kg.k
Density	680 kg/m^3
Conductivity	0.11 w/mk

PCMs with a thickness of 2 cm in June is explored in this section.

Figure 12 shows the temperature variation of the interior surface of a West wall for a typical summer day. The presence of the PCM layer causes a reduction in the peak between 2 and 5 °C. Moreover, the PCM layer causes a shift in the peak by 2 to 6 h, depending on the nature of each material candidate studied. However, the curves for the walls with PCM, will exceed that of the wall without PCM at off-peak hours. As a result, a lower heat transmission to the room and lower peak heat rate is obtained due to the lower temperature difference between the interior surface and the room temperature. The shift in the peak load make it coincide with a lower ambient temperature, consequently better performance of the cooling unit.

5.2 Effect of the PCM location

In this section, the effect of employing different types of PCMs with 2 cm thickness at west wall in June is investigated at three different positions in the wall.

- Inner PCM: where PCM locating between the brick and exterior mortar.
- Middle PCM: where PCM locating between the brick and interior mortar.
- Outer PCM: where PCM locating between the two layers of the brick.

The reduction in total quantity of heat transfer to the room and the reduction in peak heat transfer to the room due to implementing the PCMs in different locations are given in Figs. 13 and 14.

Different PCMs have different thermal characteristics. As a result, changes in thermal properties affect the amount of melted PCM which consequently affect the stored energy. As shown, the highest reduction in heat transfer is associated with PCM-5, which has the lowest thermal conductivity, among the materials under study. Therefore, this substance has a higher effect in reducing the amount of heat transfer to the room.

The results show no effect on average heat transfer for PCM-2 due to changing the PCM layer position, this is due to its low melting temperature which causes the

PCM layer to be dominated by the liquid phase almost all day at any PCM location. Such a material with low melting temperature will act as an insulation layer with fixed properties and shows no effect due to phase change.

In addition to reducing the average load, Integrating PCM material inside the building envelope will reduce and shift the peak. The effect of the PCM position is more pronounced that its effect on the average. However, there is no fixed notion toward preferring a certain position. The best position depends on the melting temperature, the latent heat of fusion, and the thermal resistance. The results show that PCM-7 has the highest reduction in peak heat flow to the room which equal to 58.52% for the outer PCM position, while PCM-1 comes in the second place in peak heat reduction by 55.67% if the PCM layer placed in the middle.

In some cases, the optimum position is neither at the inner-side nor in the outer side, as in case of PCM-1. In such case, the PCM-layer positioned at the outer side hinders the progress of the heat flux up to a certain point. After reaching complete melting, the PCM layer loses its ability to stop the heat flux. This is seen numerically in Figs. 15 and 16, near 4 PM where the results show that the outer PCM layer completely melts resulting in a surge in the cooling load.

5.3 Effect of wall orientations

The different types of phase change materials are simulated for different building façade locations North, East,

Table 4 Average and peak heat reduction at different thicknesses

PCM type	Average heat reduction [%]				Peak heat reduction [%]			
	1 cm	2 cm	3 cm	4 cm	1 cm	2 cm	3 cm	4 cm
PCM-1	6.513	12.222	17.982	23.796	34.157	55.674	63.218	67.998
PCM-2	10.503	19.007	26.035	31.944	6.896	30.34	40.731	48.973
PCM-3	10.606	19.18	26.314	32.709	27.726	52.389	64.993	70.606
PCM-4	11.136	20.049	27.327	33.42	19.921	33.597	43.997	52.138
PCM-5	23.564	38.14	48.047	55.22	31.182	49.285	60.924	68.979
PCM-6	3.99	7.636	11.019	14.174	13.562	24.672	33.873	41.427
PCM-7	10.885	19.686	26.952	33.093	43.904	57.318	64.839	69.892
PCM-8	11.04	19.862	27.042	33.03	18.721	32.778	43.664	52.246

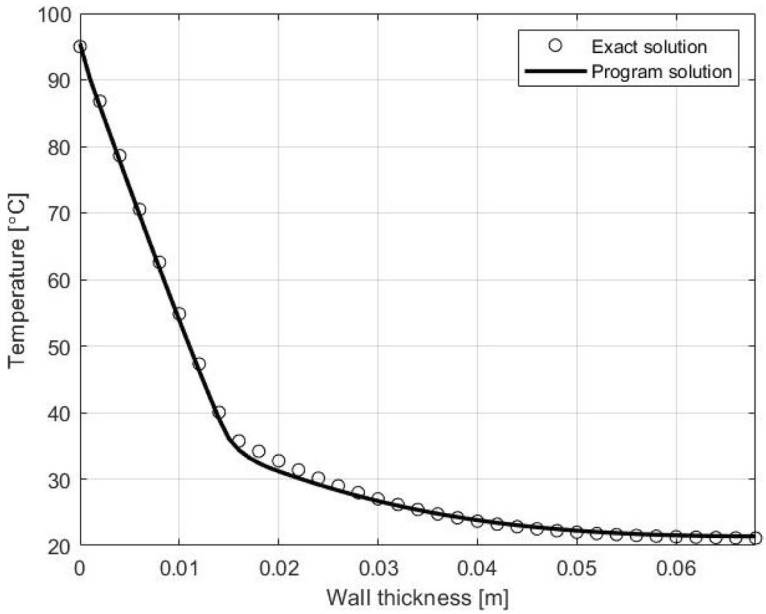

Fig. 10 Exact vs. program solution for a PCM

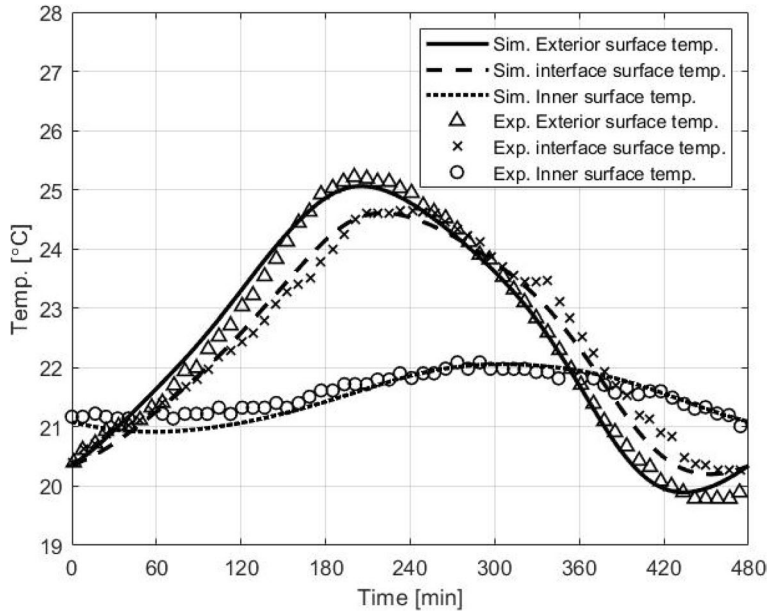

Fig. 11 Experimental results vs. simulation results

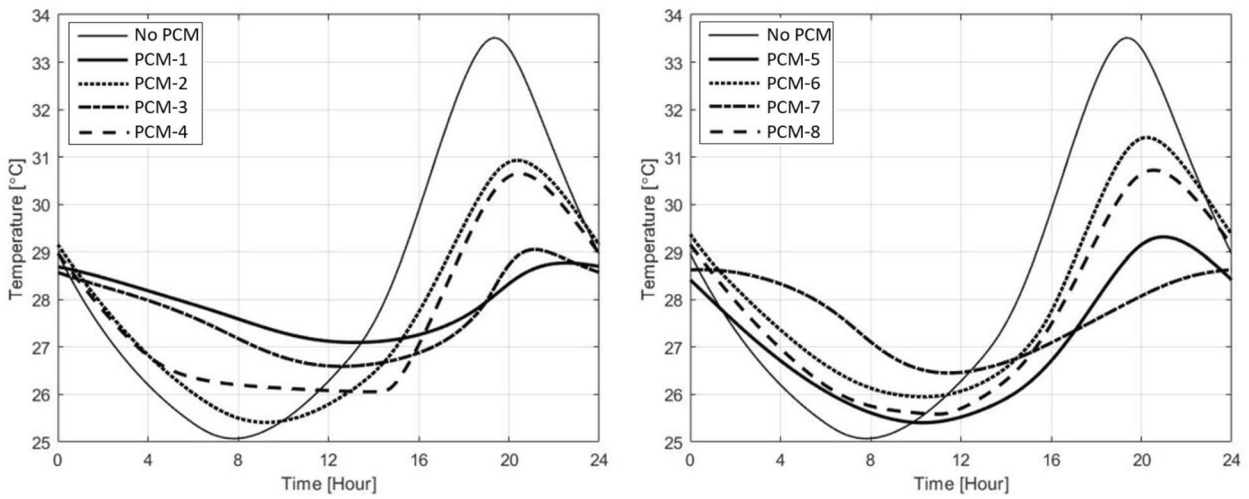

Fig. 12 Interior surface temperature variations for wall with and without PCMs

South, and West, considering middle PCM in June, the influence of the orientation of PCM wall on the reduction in average and peak heat flow to the room. The computed results are given in Fig. 17.

The results show the highest peak heat reduction for most of PCMs occurs for the west wall where the time of peak irradiance meets the peak of the ambient air temperature, which result in higher temperatures than the other orientations which enhance the effect of PCM.

5.4 The effect of PCM layer thickness

The PCM thickness was increased from 1 to 4 cm. By increasing the thickness of the PCM, the thermal resistance of the wall increased, also the quantity of energy stored rises. As a result, less energy is transferred to the room. The average and peak heat reduction for the middle PCM wall in June was calculated and the results for different thicknesses are shown in Table 4.

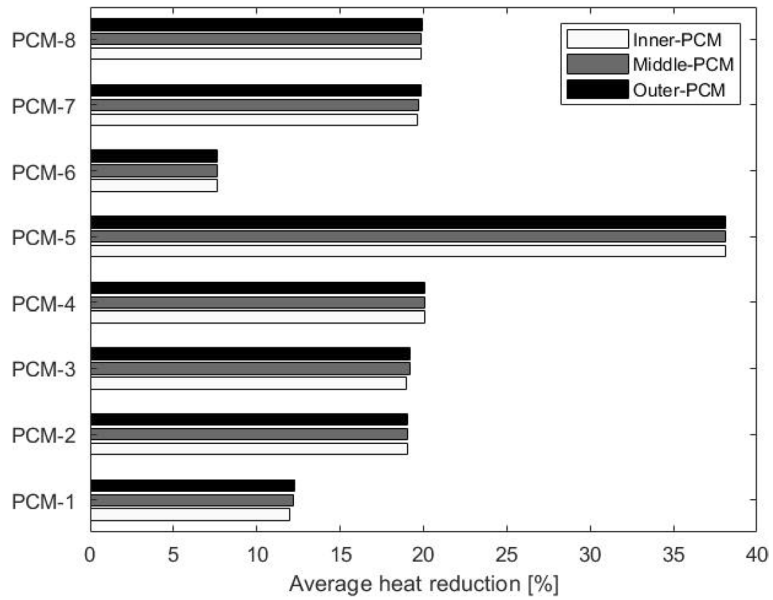

Fig. 13 Average heat reduction for different wall configurations

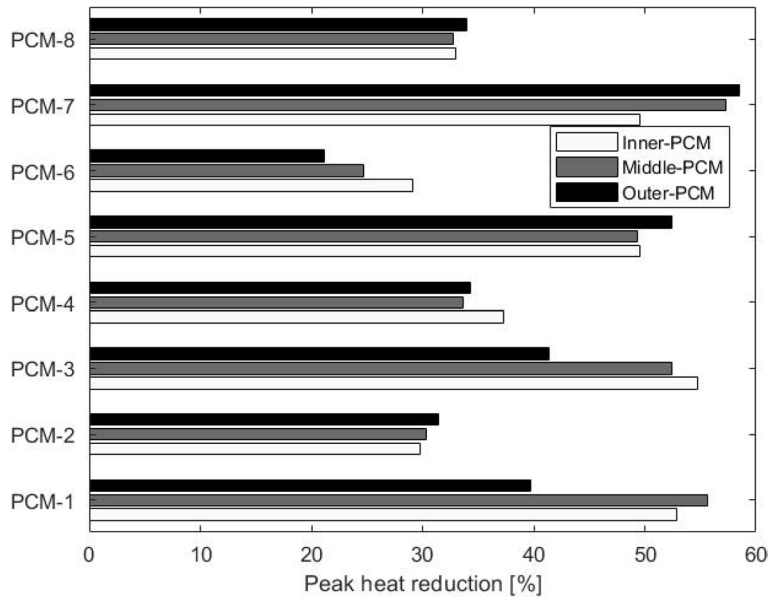

Fig. 14 Peak heat reduction for different wall configurations

The simulation results show that, regardless of the PCM type, as the PCM layer thickness increases the heat transfer to the room is decreased as the additional thickness act as a barrier to the heat transfer to the room.

5.5 The effect of seasons on the average heat transfer

To investigate the effect of changing solar radiation and the ambient temperature over the year, two months were studied, the first month was June to express the hottest month in Egypt and the second one was January to express the coldest month. Noting that the direction of heat flow is changing where the outer surface in June is higher than the room temperature, while in winter most of the day the exterior surface temperature is lower than the room temperature as shown for a base wall in Fig. 18.

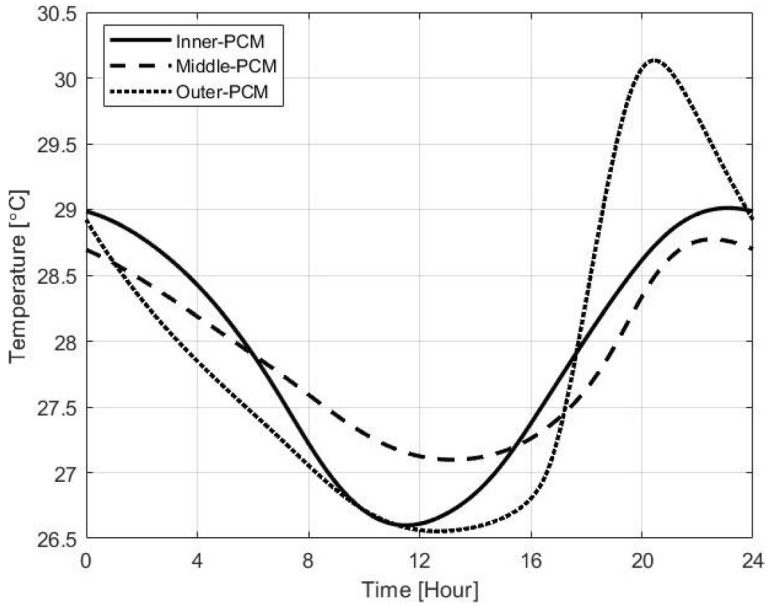

Fig. 15 Interior surface temperature variation in June for wall with PCM-1 at different configurations

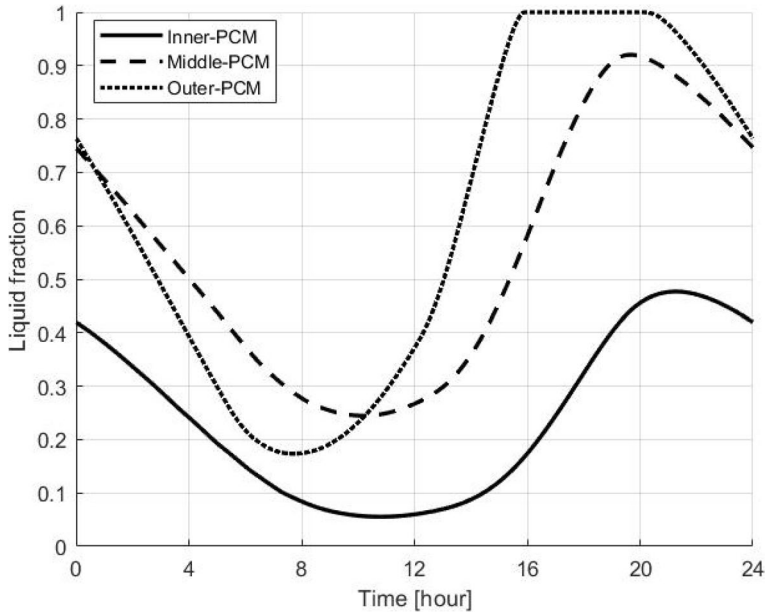

Fig. 16 Liquid fraction of PCM-1 integrated at different positions for a West wall in June

The results of average heat load reduction are given in Fig. 19, where we observed that the results in June and January were nearly identical. Noting that the average heat load reduction in June indicates that the contribution of PCM into the wall aids in reducing heat flow into the room, but the heat flow out of the room is reduced in January. This ensure the previous observation that the thermal resistance is the most dominated part on the average heat load reduction.

6 Conclusion

The construction of building envelope has a major impact on the energy consumption and consequently green-house gases emission. The effect of integrating

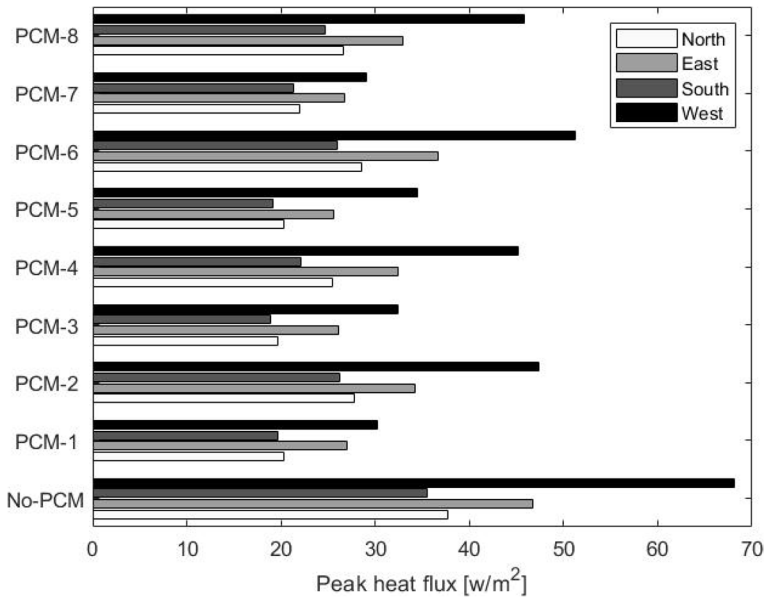

Fig. 17 Peak heat reduction for a wall at different orientations

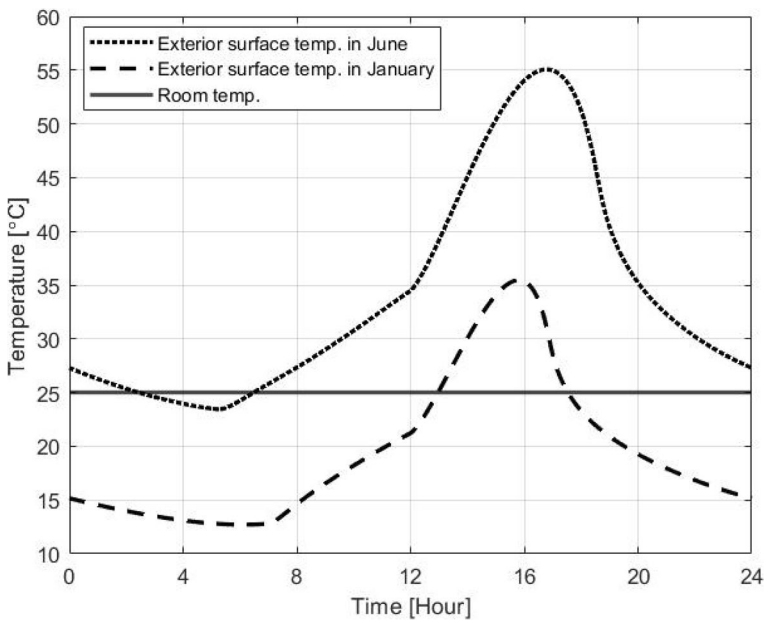

Fig. 18 Exterior surface temperature for a base wall in June and January

eight different PCMs into a base-wall construction was numerically studied. The simulations considered a number of variables, including the thickness and location of the PCM layer in the wall and the direction of the façade.

The study's general conclusions can be stated as follows:

- In general, the presence of PCMs lowers heat transfer to and from the space in the summer and winter.
- The thermal conductivity of the PCM is the most important factor to consider when choosing the right PCM. The lower the conductivity coefficient, the less heat is transferred into or out of the space in summer and winter, respectively.

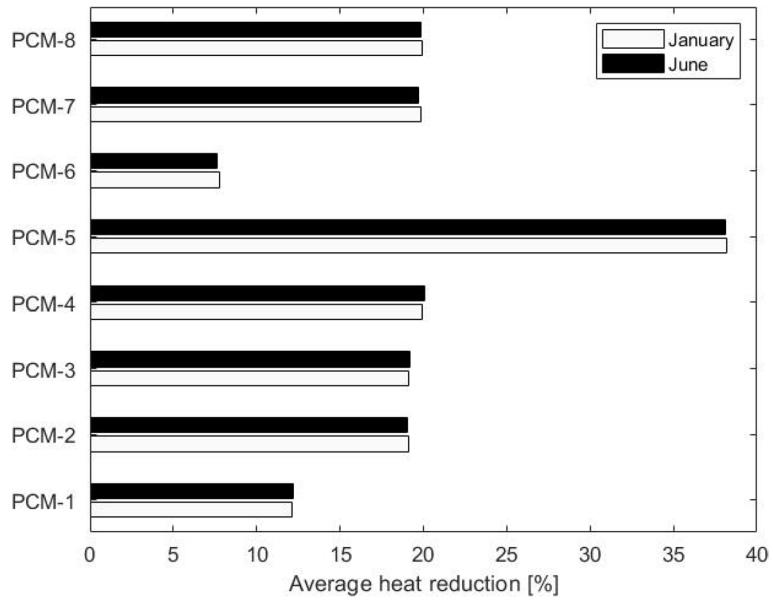

Fig. 19 Average heat reduction for different PCMs wall in June and January

- In June, PCM-5 had the best performance which reduced heat transmission by 38.136% for inner-PCM, 38.14% for middle-PCM, and 38.151% for outer-PCM.
- PCM-6, which represented the lowest performance which reduced heat transfer by 7.65% for inner-PCM, 7.636% for middle-PCM, and 7.642% for outer-PCM.
- In June, the maximum value of peak heat reduction was 58.519% for PCM-7 when it was placed as an outer PCM.
- PCM's position has a minor impact on average heat reduction but a significant impact on peak heat reduction, for all wall orientations.
- As expected, regardless of the PCM type, as the PCM layer thickness increases the average and peak heat transfer to the room is decreased.

Acknowledgements
This research has received funding for publication through the Transformative Agreement between Springer Nature and Science, Technology & Innovation Funding Authority (STDF) in cooperation with Egyptian Knowledge Bank (EKB).

Authors' contributions
Joseph Wadea has designed the MATLAB program and drafted the manuscript. Ehab Mina has been involved in drafting the manuscript and revising it critically. Ahmed Elsabbagh has been involved in revising and editing the manuscript and given final approval of the version to be published. All authors have read and agreed to the published version of the manuscript.

Funding
This research has received funding for publication through the Transformative Agreement between Springer Nature and Science, Technology & Innovation Funding Authority (STDF) in cooperation with Egyptian Knowledge Bank (EKB).

Availability of data and materials
The data that support the findings of this study are openly available.

Declarations

Competing interests
The authors declare that they have no competing interests.

Received: 18 August 2022 Accepted: 4 October 2022
Published online: 30 October 2022

References

1. Abbas, H. M., Jalil, J. M., & Ahmed, S. T. (2021). Experimental and numerical investigation of PCM capsules as insulation materials inserted into a hollow brick wall. *Energy and Buildings, 246*, 111127 https://doi.org/10.1016/J.ENBUILD.2021.111127
2. Arıcı, M., Bilgin, F., Nižetić, S., & Karabay, H. (2020). PCM integrated to external building walls: an optimization study on maximum activation of latent heat. *Applied Thermal Engineering, 165*, 114560 https://doi.org/10.1016/J.APPLTHERMALENG.2019.114560
3. Asan, H. (1998). Effects of Wall's insulation thickness and position on time lag and decrement factor. *In Energy and Buildings, 28* https://doi.org/10.1016/S0378-7788(98)00030-9
4. Baetens, R, Jelle, B. P., Thue, J. V, Tenpierik, M. J., Grynning, S., Uvsløkk, S., & Gustavsen, A. (2010). Citation for the published version (APA 6th). *Energy and Buildings*, *42*(2), 147–172. https://doi.org/10.1016/j.enbuild.2009.09.005
5. Baetens, R., Jelle, B. P., Gustavsen, A., & Grynning, S. (2010). Gas-filled panels for building applications: A state-of-the-art review. *Energy and*

Buildings, 42(11), 1969–1975 https://doi.org/10.1016/J.ENBUILD.2010.06.019
6. Bahrar, M., Djamai, Z. I., EL Mankibi, M., Si Larbi, A., & Salvia, M. (2018). Numerical and experimental study on the use of microencapsulated phase change materials (PCMs) in textile reinforced concrete panels for energy storage. *Sustainable Cities and Society, 41*, 455–468 https://doi.org/10.1016/J.SCS.2018.06.014
7. Barzin, R., Chen, J. J. J., Young, B. R., & Farid, M. M. (2015). Peak load shifting with energy storage and price-based control system. *Energy*. https://doi.org/10.1016/j.energy.2015.05.144
8. Bergman, T. L., Lavine, A. S., Incropera, F. P., & Dewitt, D. P. (2011). *Fundamentals of heat and mass transfer* (7th ed.). United States: Wiley
9. BP. (2020). *Statistical Review of World Energy globally consistent data on world energy markets.*, 66 https://www.bp.com/content/dam/bp/business-sites/en/global/corporate/pdfs/energy-economics/statistical-review/bp-stats-review-2020-full-report.pdf
10. Climate Consultant | Society of Building Science Educators. (n.d.). Retrieved June 11, 2022, from https://www.sbse.org/resources/climate-consultant
11. Dé Ric Kuznik, F., David, D., Johannes, K., & Roux, J.-J. (2010). A review on phase change materials integrated in building walls. *Renewable and Sustainable Energy Reviews, 15*, 379–391 https://doi.org/10.1016/j.rser.2010.08.019
12. Dobos, A. P. (2014). *PVWatts Version 5 Manual*. https://doi.org/10.2172/1158421
13. Duffie, J. A., & Beckman, W. A. (2013). *Solar engineering of thermal processes* (fourth ed.). *Fourth Edition* https://doi.org/10.1002/9781118671603
14. El-Ghetany, H. H., Aly, W. I. A., Shalata, H. A., Eid, A. I., & Abdelwahed, K. (2020). Experimental investigation of an energy saving system using Phase Change Materials in buildings. *Egyptian Journal of Chemistry, 63*(11), 4533–4545 https://doi.org/10.21608/EJCHEM.2020.27252.2565
15. Elrawy, O. O., & Attia, S. (2019). The impact of climate change on Building Energy Simulation (BES) uncertainty - Case study from a LEED building in Egypt. *IOP Conference Series: Earth and Environmental Science, 397*(1), 012005 https://doi.org/10.1088/1755-1315/397/1/012005
16. Figueiredo, A., Vicente, R., Lapa, J., Cardoso, C., Rodrigues, F., & Kämpf, J. (2017). Indoor thermal comfort assessment using different constructive solutions incorporating PCM. *Applied Energy, 208*, 1208–1221 https://doi.org/10.1016/j.apenergy.2017.09.032
17. Gholamibozanjani, G., & Farid, M. (2020). Peak load shifting using a price-based control in PCM-enhanced buildings. *Solar Energy, 211*, 661–673 https://doi.org/10.1016/j.solener.2020.09.016
18. Hasan, A., Al-Sallal, K. A., Alnoman, H., Rashid, Y., & Abdelbaqi, S. (2016). Effect of phase change materials (PCMs) integrated into a concrete block on heat gain prevention in a hot climate. *Sustainability (Switzerland), 8*(10) https://doi.org/10.3390/SU8101009
19. Huang, H., Zhou, Y., Huang, R., Wu, H., Sun, Y., Huang, G., & Xu, T. (2020). Optimum insulation thicknesses and energy conservation of building thermal insulation materials in Chinese zone of humid subtropical climate. *Sustainable Cities and Society, 52*, 101840 https://doi.org/10.1016/J.SCS.2019.101840
20. Kalnaes, S. E., & Jelle, B. P. (2014). *Vacuum insulation panel products: a state-of-the-art review and future research pathways.* https://doi.org/10.1016/j.apenergy.2013.11.032
21. Kenisarin, M. M. (2014). Thermophysical properties of some organic phase change materials for latent heat storage. A review. *SOLAR ENERGY, 107*, 553–575 https://doi.org/10.1016/j.solener.2014.05.001
22. Khan, R. J., Bhuiyan, M. Z. H., & Ahmed, D. H. (2020). Investigation of heat transfer of a building wall in the presence of phase change material (PCM). *Energy and Built Environment, 1*(2), 199–206 https://doi.org/10.1016/J.ENBENV.2020.01.002
23. Kharbouch, Y., Ouhsaine, L., Mimet, A., & El Ganaoui, M. (2018). Thermal performance investigation of a PCM-enhanced wall/roof in northern Morocco. *Building Simulation, 11*(6), 1083–1093 https://doi.org/10.1007/S12273-018-0449-5
24. Kumarasamy, K., An, J., Yang, J., & Yang, E.-H. (2016). Numerical techniques to model conduction dominant phase change systems: a CFD approach and validation with DSC curve. *Energy & Buildings*. https://doi.org/10.1016/j.enbuild.2016.02.040
25. Lee, K. O., Medina, M. A., Sun, X., & Jin, X. (2018). Thermal performance of phase change materials (PCM)-enhanced cellulose insulation in passive solar residential building walls. *Solar Energy, 163*, 113–121 https://doi.org/10.1016/J.SOLENER.2018.01.086
26. Li, Z. X., Al-Rashed, A. A. A. A., Rostamzadeh, M., Kalbasi, R., Shahsavar, A., & Afrand, M. (2019). Heat transfer reduction in buildings by embedding phase change material in multi-layer walls: effects of repositioning, thermophysical properties and thickness of PCM. *Energy Conversion and Management, 195*, 43–56 https://doi.org/10.1016/J.ENCONMAN.2019.04.075
27. Medveď, I., Trník, A., & Vozár, L. (2016). *Modeling of a heat capacity peak and an enthalpy jump for a paraffin-based phase-change material*.
28. Meng, E., Yu, H., Zhan, G., & He, Y. (2013). Experimental and numerical study of the thermal performance of a new type of phase change material room. *Energy Conversion and Management, 74*, 386–394 https://doi.org/10.1016/j.enconman.2013.06.004
29. Molinari, C., Zanelli, C., Laghi, L., De Aloysio, G., Santandrea, M., Guarini, G., Conte, S., & Dondi, M. (2021). Effect of scale-up on the properties of PCM-impregnated tiles containing glass scraps. *Case Studies in Construction Materials, 14*, e00526 https://doi.org/10.1016/J.CSCM.2021.E00526
30. Saikia, P., Azad, A. S., & Rakshit, D. (2018). Thermodynamic analysis of directionally influenced phase change material embedded building walls. *International Journal of Thermal Sciences, 126*, 105–117 https://doi.org/10.1016/J.IJTHERMALSCI.2017.12.029
31. Sam, M. N., Caggiano, A., Mankel, C., & Koenders, E. (n.d.). *Materials a comparative study on the thermal energy storage performance of bio-based and paraffin-based PCMs using DSC procedures*. https://doi.org/10.3390/ma13071705
32. Saxena, R., Biplab, K., & Rakshit, D. (2018). Quantitative assessment of phase change material utilization for building cooling load abatement in composite climatic condition. *Journal of Solar Energy Engineering, Transactions of the ASME, 140*(1) https://doi.org/10.1115/1.4038047
33. Shilei, L., Neng, Z., & Guohui, F. (2006). Impact of phase change wall room on indoor thermal environment in winter. *Energy and Buildings, 38*(1), 18–24 https://doi.org/10.1016/J.ENBUILD.2005.02.007
34. Simmler, H., & Brunner, S. (n.d.). *Vacuum insulation panels for building application Basic properties, aging mechanisms and service life*. https://doi.org/10.1016/j.enbuild.2005.06.015
35. Soares, N., Gaspar, A. R., Santos, P., & Costa, J. J. (2014). Multi-dimensional optimization of the incorporation of PCM-drywalls in lightweight steel-framed residential buildings in different climates. *Energy and Buildings, 70*, 411–421 https://doi.org/10.1016/J.ENBUILD.2013.11.072
36. Solomon, A. D. (1979). An easily computable solution to a two-phase Stefan problem. *Solar Energy, 23*(6), 525–528 https://doi.org/10.1016/0038-092X(79)90077-X
37. Sovetova, M., Memon, S. A., & Kim, J. (2019). Thermal performance and energy efficiency of building integrated with PCMs in hot desert climate region. *Solar Energy, 189*, 357–371 https://doi.org/10.1016/J.SOLENER.2019.07.067
38. Tenpierik, M., Wattez, T., & M., Cosmatu, T. E., & Tsafou, S. (2019). Temperature control in (translucent) phase change materials applied in facades: a numerical study. *Energies, 12*, 3286 https://doi.org/10.3390/en12173286
39. Thiele, A. M., Wei, Z., Falzone, G., Young, B. A., Neithalath, N., Sant, G., & Pilon, L. (2016). *Figure of merit for the thermal performance of cementitious composites containing phase change materials*. https://doi.org/10.1016/j.cemconcomp.2015.10.023
40. Tyagi, V. V, Pandey, A. K., Buddhi, D., & Kothari, R. (2016). *Title: Thermal performance assessment of encapsulated PCM based thermal management system to reduce peak energy demand in Buildings*. https://doi.org/10.1016/j.enbuild.2016.01.042
41. United Nations Environment Programme. (2022). Buildings and climate change: summary for decision makers. https://www.unep.org/
42. Vik, T., Madessa, H., Chaudhuri, A., Aamodt, A., & Phengphan, C. (2020). *Experimental and numerical studies on thermal performance of an office cubicle having gypsum boards coated with PCM-enhanced spackling*.
43. Voelker, C., Kornadt, O., & Ostry, M. (2008). Temperature reduction due to the application of phase change materials. *Energy and Buildings, 40*(5), 937–944 https://doi.org/10.1016/J.ENBUILD.2007.07.008

44. Xiong, T., Wang, Y., & Yang, X. (2017). Numerical investigation of dynamic melting process in a thermal energy storage system using U-tube heat exchanger. *Special Issue Article Advances in Mechanical Engineering, 9*(5), 1–10 https://doi.org/10.1177/1687814017707415

Publisher's Note